

Examining the Noncompetitive Antagonist-binding Site in the Ion Channel of the Nicotinic Acetylcholine Receptor in the Resting State*

(Received for publication, June 15, 1999, and in revised form, November 1, 1999)

Michael P. Blanton^{‡§}, Elizabeth A. McCarty[‡], and Martin J. Gallagher[¶]

From the [‡]Departments of Pharmacology and Anesthesiology, Texas Tech University Health Sciences Center, Lubbock, Texas 79430 and [¶]Department of Neurology, Washington University School of Medicine, St. Louis, Missouri 63110

3-Trifluoromethyl-3-(*m*-[¹²⁵I]iodophenyl)diazirine ([¹²⁵I]TID) has been shown to be a potent noncompetitive antagonist (NCA) of the nicotinic acetylcholine receptor (AChR). Amino acids that contribute to the binding site for [¹²⁵I]TID in the ion channel have been identified in both the resting and desensitized state of the AChR (White, B. H., and Cohen, J. B. (1992) *J. Biol. Chem.* 267, 15770–15783). To characterize further the structure of the NCA-binding site in the resting state channel, we have employed structural analogs of TID. The TID analogs were assessed by the following: 1) their ability to inhibit [¹²⁵I]TID photoincorporation into the resting state channel; 2) the pattern, agonist sensitivity, and NCA inhibition of [¹²⁵I]TID analog photoincorporation into AChR subunits. The addition of a primary alcohol group to TID has no demonstrable effect on the interaction of the compound with the resting state channel. However, conversion of the alcohol function to acetate, isobutyl acetate (TIDBIBA), or to trimethyl acetate leads to rightward shifts in the concentration-response curves for inhibition of [¹²⁵I]TID photoincorporation into the AChR channel and a progressive reduction in the agonist sensitivity of [¹²⁵I]TID analog photoincorporation into AChR subunits. Inhibition of [¹²⁵I]TID analog photoincorporation by NCAs (e.g. tetracaine) as well as identification of the sites of [¹²⁵I]TIDBIBA photoincorporation in the δ M2 segment indicate a common binding locus for each TID analog. We conclude that relatively small additions to TID progressively reduce its ability to interact with the NCA site in the resting state channel. A model of the NCA site and resting state channel is presented.

Noncompetitive antagonists (NCAs)¹ of the nicotinic acetylcholine receptor (AChR) are by definition agents that block the

permeability response of the receptor by binding to sites that are distinct from the agonist-binding sites (recent reviews include Refs. 1–3). NCAs of the AChR are a large and structurally heterogeneous group of compounds that include local anesthetics, long chain alcohols, barbiturates, phencyclidine, ethidium, substance P, and insecticides (4). Noncompetitive antagonists used as photoaffinity probes of the AChR were instrumental in determining that the transmembrane α -helical M2 segment of each receptor subunit forms the lining of the ion channel pore (5–9). Under equilibrium binding conditions, the majority of NCAs interact preferentially with the AChR when acetylcholine sites are occupied by agonist, that is they bind preferentially to the desensitized state of the AChR. Photoaffinity labeling studies with NCAs have identified several unique binding loci within the channel of the AChR in the desensitized state (5–10). Examples of NCAs such as the local anesthetic tetracaine (11, 12) and the compound diazofluorene (13), which bind with appreciable (micromolar) affinity to the AChR channel when agonist is not bound to the receptor, which is in the resting state, are far less prevalent.

The uncharged, photoreactive compound 3-trifluoromethyl-3-(*m*-[¹²⁵I]iodophenyl)diazirine ([¹²⁵I]TID) is another NCA that interacts with high affinity with the AChR channel in the resting state. TID is a potent noncompetitive antagonist of the AChR, inhibiting agonist-induced ion flux and binding with micromolar affinity to the channel in both the resting and desensitized states (14, 15). TID is a unique compound in that there are two components to its photoincorporation into the AChR. First, TID is a potent NCA, and one component of [¹²⁵I]TID photoincorporation is localized to the channel-lining M2 segments of each receptor subunit. [¹²⁵I]TID photoincorporation into the M2 segment of each AChR subunit is inhibited in a concentration-dependent manner by TID itself as well as by other noncompetitive antagonists (14, 16, 17). In addition to “specific” photoincorporation into amino acids in the M2 segments of each AChR subunit, [¹²⁵I]TID also photoincorporates into amino acids in the M1, M3, and M4 transmembrane segments of each receptor subunit. The extent of [¹²⁵I]TID photoincorporation into residues in the M1, M3, and M4 segments is not affected by the further addition of an excess of nonradioactive TID or other noncompetitive antagonists, that is the labeling is “nonspecific.” Consistent with the hydrophobic nature of TID, it partitions extremely effectively into the lipid bilayer, and [¹²⁵I]TID photoincorporation into amino acids in the transmembrane segments M1, M3, and M4 is interpreted as indicating that these residues are situated at the lipid-protein interface of the AChR (18–20).

methoxybenzoic acid 8-(diethylamino) octyl ester; MOPS, 4-morpholinopropanesulfonic acid.

* This work was supported in part by NINDS Grant R29 NS35786 from the National Institutes of Health. The costs of publication of this article were defrayed in part by the payment of page charges. This article must therefore be hereby marked “advertisement” in accordance with 18 U.S.C. Section 1734 solely to indicate this fact.

§ To whom correspondence should be addressed: Dept. of Pharmacology, Texas Tech University Health Sciences Center, 3601 4th St., Lubbock, TX 79430. Tel.: 806-743-2425; Fax: 806-743-2744; E-mail: phrmpb@ttuhsc.edu.

¹ The abbreviations used are: NCA, noncompetitive antagonist; AChR, nicotinic acetylcholine receptor; [³H]TCP, [³H]thienyl-cyclohexylpiperidine; [¹²⁵I]TID, 3-trifluoromethyl-3-(*m*-[¹²⁵I]iodophenyl)diazirine; TTDBA, TTDBAc, TTDBIBA, TTDBTMAc, TTD-BE 4'-(3-trifluoromethyl-3*H*-diazirine-3-yl)-2'-tributylstannybenzyl (alcohol, acetate, isobutyric acetate, trimethyl acetate, benzoate); DMAP, 4-(dimethylamino)pyridine; PAGE, polyacrylamide gel electrophoresis; Tricine, *N*-[2-hydroxy-1,1-bis(hydroxymethyl)ethyl]glycine; HPLC, high performance liquid chromatography; PTH, phenylthiohydantoin; TMB-8, 3,4,5-tri-

Whereas TID binds with micromolar affinity to the AChR channel in both the resting and desensitized state (14), [125 I]TID photoincorporates into amino acids in the M2 segment of each AChR subunit in the resting state with 10-fold greater efficiency than in the desensitized state. In the resting state, [125 I]TID reacts with homologous aliphatic residues in each M2 segment that are located 9 and 13 amino acid residues carboxyl-terminal to the conserved lysine residue at the amino terminus of the M2 region (e.g. δ Leu-265 and δ Val-269). These results provide important information about the NCA-binding site and suggest that the conserved leucine residues at position 9 (e.g. δ Leu-265) may form a permeability barrier to the passage of ions in the resting state channel (16).

The work presented here employs analogs of TID to examine further the molecular determinants of the NCA-binding site in the AChR channel in the resting state. The interaction of TID analogs with the NCA-binding site in the resting state channel were assessed in several ways as follows: 1) the ability of nonradioactive TID analogs to inhibit [125 I]TID photoincorporation into the M2 segments of the resting state channel; 2) the pattern and agonist sensitivity of [125 I]TID analog photoincorporation into AChR subunits in the resting state, as well as direct identification of the binding site of the TID analog, TID-benzylisobutylacetate ([125 I]TIDBIBA); 3) the ability of NCAs that interact with the resting state channel to inhibit competitively photoincorporation of [125 I]TID analogs into AChR subunits in the resting state. We found that the addition of a primary alcohol group to TID (position 1 of the benzene ring; TIDBA) has no significant effect on the interaction of the compound with the resting state channel. However, conversion of the alcohol function to acetate, isobutyl acetate, or to trimethyl acetate (TIDBAC, TIDBIBA, or TIDBTMAC) leads to rightward shifts (decreased potency) in the [125 I]TID inhibition concentration-response curves and a progressive reduction in the agonist sensitivity of [125 I]TID analog photoincorporation into AChR subunits. In addition, the ability of NCAs such as tetracaine to inhibit competitively [125 I]TID analog photoincorporation into AChR subunits as well as the determination that the sites of [125 I]TIDBIBA photoincorporation within the δ M2 segment are identical to those of [125 I]TID indicate that each of the TID analogs binds to a single site in the resting state channel. We conclude that relatively small structural additions to TID result in a progressive reduction in the TID analogs ability to bind to and photolabel the NCA site in the resting state channel. The structure-activity studies with TID analogs and the AChR lead us to suggest a model for the structure of the resting state channel and the NCA-binding site.

EXPERIMENTAL PROCEDURES

Materials—AChR-rich membranes were isolated from *Torpedo californica* electric organ (21). Reactivials were purchased from Pierce, silica gel 60 thin layer chromatography (TLC) plates from Merck, and Na 125 I and [3 H]TCP (55 Ci/mmol) from NEN Life Science Products. [125 I]TID (~10 Ci/mmol) was purchased from Amersham Pharmacia Biotech and stored in 75% ethanol at 4 °C. Organic chemicals including acetic anhydride, isobutyric anhydride, trimethylacetic anhydride, and 4-(dimethylamino)pyridine (DMAP) were obtained from Aldrich. Amobarbital, pentobarbital, tetracaine, 3,4,5-trimethoxybenzoic acid 8-(diethylamino)octyl ester (TMB-8), and α -bungarotoxin were purchased from Sigma and Research Biochemicals. L-1-Tosylamido-2-phenylethyl chloromethyl ketone-treated trypsin came from Worthington, *Staphylococcus aureus* V8 protease from ICN, and Genapol C-100 (10%) from Calbiochem. Prestained low molecular weight gel standards were purchased from Life Technologies, Inc.

TID Analogs—[125 I]TIDBA and [125 I]TID-BE (Fig. 1) were prepared by radioiododestannylation of the tin-based precursors 4'-(3-trifluoromethyl-3H-diazirin-3-yl)-2'-tributylstannylbenzyl alcohol (TTDBA) and 4'-(3-trifluoromethyl-3H-diazirin-3-yl)-2'-tributylstannylbenzyl benzoate (TTD-BE), respectively (10, 22, 23). The tin-based precursors were a generous gift from Dr. Josef Brunner of the Swiss Federal Institute of

Technology (ETH), Zurich, Switzerland. Briefly, 45 nmol of TTDBA or TTD-BE in ethanol/toluene (1:1) were added to a 1-ml Reactivial and dried under nitrogen. The dried material was dissolved in 20 μ l of acetic acid, 2 mCi of Na 125 I was then added, and the iodination reaction initiated by the further addition of 5 μ l of peracetic acid. After 15 min the reaction was quenched by adding 3 μ l of NaI (100 mM) and 200 μ l of sodium bisulfite (10% (w/w)). The radiiodinated compound was extracted into 400 μ l of ethyl acetate (upper phase), which was removed and dried under nitrogen. The dried material was dissolved in 100 μ l of ethanol/toluene (1:1), applied to a Silica Gel 60 TLC plate (5 \times 20 cm), and developed with ether/hexane (1:9). The positions of [125 I]TIDBA or [125 I]TID-BE were determined by autoradiography. [125 I]TIDBA (R_f = 0.25) and [125 I]TID-BE (R_f = 0.74) were scraped from the TLC plate, extracted with 1 ml of ethanol, dried under nitrogen, dissolved in 50 μ l of ethanol and stored at -20 °C. Nonradioactive stocks of TIDBA and TID-BE were made in nearly identical fashion, and the concentrations were determined spectrophotometrically ($\epsilon_{351\text{ nm}} = 450$ (22)). The TID analogs TTDBAc, TTDBIBA, and TTDBTMAc were made by acylation of the alcohol function of the tin precursor TTDBA (22). Briefly, 20 μ l of TTDBA (1.8 μ mol) was added to a 300- μ l Reactivial, the solvent removed by a stream of N $_2$ gas, and 4 μ mol of 4-(dimethylamino)pyridine (DMAP) and 100 μ l of anhydrous tetrahydrofuran added. Under anhydrous conditions, 50 μ mol of either acetic anhydride, isobutyric anhydride, or trimethylacetic anhydride were added, and the acylation reaction was allowed to proceed overnight at room temperature (in the dark). Following solvent evaporation and resuspension in ethanol, each of the tin precursors were purified by TLC (ether/hexane, 1:9), TTDBAc (R_f = 0.58), TTDBIBA (R_f = 0.72), and TTDBTMAc (R_f = 0.78). The concentration of each purified tin precursor was checked spectrophotometrically ($\epsilon_{364\text{ nm}} = 450$). [125 I]TIDBAC, [125 I]TIDBIBA, and [125 I]TIDBTMAc (Fig. 1) as well as nonradioactive analogs were produced from the corresponding tin precursor and purified in a fashion identical to that described above for [125 I]TIDBA.

Photolabeling of AChR-rich Membranes with [125 I]TID Analogs—For labeling experiments, *Torpedo* AChR-rich membranes (1 mg/ml in Vesicle Dialysis Buffer (VDB), 10 mM MOPS, 100 mM NaCl, 0.1 mM EDTA, and 0.02% NaN $_3$, pH 7.5) were incubated for 2 h at room temperature with either [125 I]TID, [125 I]TIDBA, [125 I]TIDBAC, [125 I]TIDBIBA, or [125 I]TIDBTMAc at a final concentration of ~1.6 μ M (0.4 μ M for [125 I]TID) and with or without 400 μ M carbamylcholine chloride or drugs at various concentrations (see text). For analytical labeling experiments, approximately 1 mg of AChR membranes were used and 10 mg (per condition) for preparative labelings. Incubations were performed in either glass test tubes or vials and under reduced lighting conditions. The samples were then irradiated with a 365 nm UV lamp (Spectroline EN-280L) for 7 min at a distance of less than 1 cm and centrifuged at 39,000 $\times g$ for 1 h. Pellets were solubilized in electrophoresis sample buffer and subjected to SDS-PAGE (24).

For analytical labelings 1.0-mm thick SDS-PAGE gels were used (1.5-mm thick for preparative labeling experiments) containing separating gels composed of 8% polyacrylamide, 0.33% bisacrylamide. Following electrophoresis, gels were stained with Coomassie Blue R-250 to visualize AChR subunit bands. Analytical gels were dried and exposed to Kodak X-Omat LS film with an intensifying screen at -80 °C (1-3-day exposure). Preparative gels and analytical gels for which receptor subunits were to be subjected to proteolytic mapping were soaked in distilled water overnight, and the bands for α -, β -, γ -, and δ -subunits excised from the 8% gels. Proteolytic mapping of the sites of [125 I]TID analog photoincorporation within AChR subunits was performed according to the method of Cleveland *et al.* (25) and as described in detail in Blanton *et al.* (10). For preparative gels, AChR subunits were eluted from the excised gel pieces into 15 ml of Elution Buffer (0.1 M NH $_4$ HCO $_3$, 0.1% (w/v) SDS, 1% β -mercaptoethanol, pH 7.8) for 4 days at room temperature with gentle mixing. The gel suspensions were then filtered through Whatman No. 1 paper and concentrated using a Centrprep-10 (Amicon). Excess SDS was removed by acetone precipitation (~85% acetone at -20 °C for 12 h).

For analytical labeling experiments, [125 I]TID photoincorporation into AChR subunits was quantified by cutting out the receptor bands from the dried 8% acrylamide gel and determining the amount of [125 I]cpm present in each band by γ -counting in a Packard Cobra II gamma counter (10 min counting time/band). For [125 I]TID analog competition labeling experiments (Figs. 2 and 4), the data points were determined according to Equation 1.

% specific [125 I]TID analog photoincorporation into AChR γ -subunit =

$$\frac{(\text{cpm}_{[\text{drug}]} - \text{cpm}_{[\text{carb}]})}{(\text{cpm}_{[\text{control}]} - \text{cpm}_{[\text{carb}]})} \times 100 \quad (\text{Eq. 1})$$

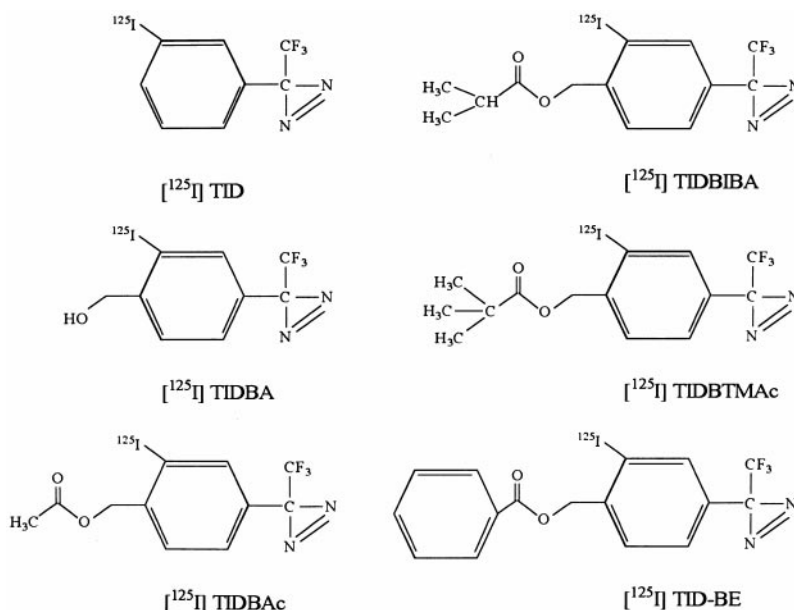


FIG. 1. Structures of the ^{125}I TID analogs.

The $\text{cpm}_{[\text{drug}]}$ is the amount of ^{125}I TID analog photoincorporation into the AChR γ -subunit at a given concentration of drug; $\text{cpm}_{[\text{carb}]}$ is the amount of ^{125}I TID analog incorporated into the γ -subunit in the presence of the agonist carbamylcholine, and $\text{cpm}_{[\text{control}]}$ is the amount of ^{125}I TID analog incorporated into the γ -subunit in the absence of any other ligand. Subtracting the $\text{cpm}_{[\text{control}]}$ from the $\text{cpm}_{[\text{carb}]}$ restricts the ^{125}I TID analog labeling to that which is specifically localized to the channel-lining M2 segment (14, 16, 17). The concentration-response data were curve-fitted by nonlinear least squares analysis (one-site competition) using the graphical curve-fitting program Prism (Graphpad).

Isolation of ^{125}I TIDBIBA-photolabeled M2-containing Fragment of the AChR δ -Subunit—AChRs were photolabeled with ^{125}I TIDBIBA (10 mg of AChR-rich membranes per labeling condition) under conditions that favor either the resting state or the desensitized state (*i.e.* in the presence of the agonist carbamylcholine). AChR subunits were resolved on 1.5-mm thick 8% acrylamide gels, and the δ -subunit was isolated as described above. For digestion with trypsin, acetone-precipitated δ -subunits were resuspended in approximately 300 μl of 0.1 M NH_4HCO_3 , 0.02% (w/v) SDS, 0.5% Genapol C-100, pH 7.8 (1–2 mg/ml protein). Trypsin was added at a 20% (w/w) enzyme to substrate ratio, and the digestion was allowed to proceed 4–5 days at room temperature. A small aliquot of each sample was electrophoresed on an analytical (1.0-mm thick) 16.5% T, 6% C Tricine SDS-PAGE gel with at least one reference lane containing prestained low molecular weight protein standards (Life Technologies, Inc). The Tricine gel was stained, destained, and dried for autoradiography. The bulk of the δ -subunit tryptic digests were solubilized in electrophoresis sample buffer and submitted to preparative (1.5-mm thick) scale 16.5% T, 6% C Tricine gel analysis (10, 13, 16). Preparative Tricine gels were stained, destained, and soaked in water overnight. By using the autoradiograph from the analytical Tricine gel in conjunction with the prestained protein standards, an approximately 5-kDa band known to contain the M2 segment of the δ -subunit ($\delta\text{T-5K}$ (13, 16)) was excised from the gel and eluted into 4 ml of Elution Buffer for 4 days at room temperature. The $\delta\text{T-5K}$ fragment was further purified by reverse-phase HPLC using a Brownlee Aquapore C_4 column (100 \times 2.1 mm) with Solvent A (0.08% trifluoroacetic acid in water) and Solvent B (0.05% trifluoroacetic acid in 60% acetonitrile, 40% 2-propanol). A nonlinear elution gradient was employed (25–100% Solvent B in 80 min), and the elution of peptides was monitored by the absorbance at 210 nm. Collected fractions were counted for radioactivity, and the peak protein/radioactivity-containing fractions were pooled, dried by vacuum centrifugation, and resuspended in 20 μl of 0.1 M NH_4HCO_3 , 0.1% (w/v) SDS, pH 7.8, for protein radiosequence analysis.

Sequence Analysis—Amino-terminal sequence analysis was performed on a Beckman Instruments (Porton) model 20/20 protein sequencer using gas phase cycles (Texas Tech University Biotechnology Core Facility). Peptide aliquots (25 μl) were immobilized on chemically modified glass fiber disks (Beckman Instruments), which were used to

improve the sequencing yields of hydrophobic peptides. Approximately 20% of the release PTH-derivatives were separated by an on-line PTH-derivative analyzer, and approximately 80% was collected for determination of released ^{125}I cpm by γ -counting of each sample for 20 min. Initial yield (I_0) and repetitive yield (R) were calculated by nonlinear least squares regression of the observed release (M) for each cycle (n): $M = I_0 R^n$ (PTH-derivatives of Cys and His were omitted from the fit).

RESULTS

TID Analog Inhibition of ^{125}I TID Photoincorporation into the AChR Channel in the Resting State—In these studies, we wished to examine the molecular determinants of ^{125}I TID interaction with the AChR channel in the resting state. Non-radioactive analogs of TID (Fig. 1) were first constructed, and their ability to inhibit ^{125}I TID photoincorporation into the resting state channel was tested. In the absence of agonist (resting state AChR), the majority (>75%) of ^{125}I TID photoincorporation into individual AChR subunits reflects labeling of amino acid residues in the M2 transmembrane segment, with the M2 segment of each subunit collectively constituting the resting state channel (14, 16). Addition of the AChR agonist carbamylcholine, or NCAs such as tetracaine or TMB-8, reduces by greater than 75% the photoincorporation of ^{125}I TID into receptor subunits (16, 17), reflecting an identical reduction in the extent of ^{125}I TID photoincorporation into amino acids in the M2 segment of each receptor subunit.

To assay the effect of each TID analog on ^{125}I TID photoincorporation into the resting state channel, AChR-rich membranes were equilibrated in the absence of agonist with ^{125}I TID and increasing concentrations of a given TID analog. Following UV irradiation and SDS-PAGE, all four AChR subunits are labeled (Fig. 2A) with the extent of ^{125}I TID photoincorporation into the γ -subunit \sim 4-fold greater than that into the α -, β -, or δ -subunits (Fig. 2A, 1st lane). Addition of agonist alone (400 μM carbamylcholine) decreased the extent of ^{125}I TID photoincorporation into each receptor subunit of the desensitized state AChR by 75% or greater (93% reduction for γ -subunit; Fig. 2A, 8th lane). As shown representatively by the isobutylacetate analog of TID (TIDBIBA; Fig. 2A, 2nd to 7th lanes), each TID analog tested reduced the extent of ^{125}I TID photoincorporation into receptor subunits in a concentration-dependent fashion.

The concentration dependence of the reduction of ^{125}I TID photoincorporation into AChR subunits by each TID analog was quantified by excising the individual AChR subunit bands

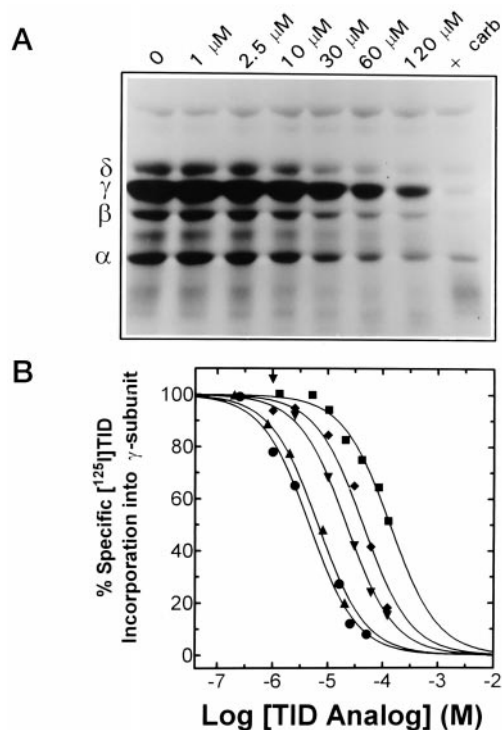


FIG. 2. The effect of TID analogs on the photoincorporation of $[^{125}\text{I}]\text{TID}$ into AChR-rich membranes. AChR-rich membranes were equilibrated (2 h) with $[^{125}\text{I}]\text{TID}$ ($0.4 \mu\text{M}$) in the absence (1st–7th lanes) and in the presence (8th lane) of $400 \mu\text{M}$ carbamylcholine (agonist) or in the presence of increasing concentrations of each of the TID analogs shown in Fig. 1 (2nd to 7th). AChR-rich membranes were then irradiated at 365 nm for 7 min, and polypeptides were resolved by SDS-PAGE. A, shown is the corresponding autoradiograph of the gel containing the competition labeling experiment $[^{125}\text{I}]\text{TID}$ versus TIDBIBA (0, 1, 2.5, 10, 30, 60, 120 μM). The positions of the AChR subunits are indicated on the left. B, for each $[^{125}\text{I}]\text{TID}$ competition labeling experiment, individual AChR subunit bands were excised from the dried gel, and the amount of $[^{125}\text{I}]\text{TID}$ incorporated into each subunit was determined by gamma counting. The data points for $[^{125}\text{I}]\text{TID}$ photoincorporation into the AChR γ -subunit are shown and were calculated as described under “Experimental Procedures.” The solid lines represent the nonlinear least-squares fit of each of the binding data sets. The IC_{50} values calculated from these curves are shown in Table I. TIDBA (●), TIDBAc (▲), TIDBIBA (▼), TIDBTMAc (◆), TID-BE (■).

from the dried polyacrylamide gel and determining the amount of ^{125}I cpm present by γ -counting. The extent of $[^{125}\text{I}]\text{TID}$ photoincorporation into receptor subunits in the presence of high concentrations of NCAs (including TID itself) compared with photoincorporation in the presence of carbamylcholine alone shows no difference (data not shown (14, 17)); therefore, the amount of $[^{125}\text{I}]\text{TID}$ photoincorporation into subunits of the desensitized state AChR was used to define the level of non-specific photoincorporation. The amount of $[^{125}\text{I}]\text{TID}$ photoincorporation in the presence of drug (TID analog) was then calculated as a percentage of the total agonist-inhibitable specific labeling. Concentration-response curves for each TID analog are shown in Fig. 2B, and the calculated IC_{50} values are presented in Table I. The alcohol and acetate analogs of TID (Fig. 1; TIDBA and TIDBAc) were the most potent inhibitors of $[^{125}\text{I}]\text{TID}$ photoincorporation into AChR subunits in the resting state with IC_{50} values approximating that of TID itself. The addition of either two or three methyl groups to the acetate function of TIDBAc (yielding TIDBIBA and TIDBTMAc) resulted in 3.5- and 7.3-fold decreases in potency, respectively. Finally, compared with TIDBA, the analog TID-BE had a nearly 30-fold reduced potency for inhibition of $[^{125}\text{I}]\text{TID}$ photoincorporation into the resting state channel.

TABLE I

Calculated IC_{50} values for drug blockage of $[^{125}\text{I}]\text{TID}$ photoincorporation into the resting state AChR γ -subunit

The IC_{50} values (concentration at which drug reduces $[^{125}\text{I}]\text{TID}$ photoincorporation into the γ -subunit of the AChR by 50% of the maximal effect) were determined by nonlinear least squares analysis. $[^{125}\text{I}]\text{TID}$ labeling of the resting state of the AChR is described under “Experimental Procedures.”

TID analog	IC_{50}	
	γ -Subunit	($\alpha\beta\gamma\delta$ Subunit average)
	μM	
TID	4 ^a	4 ^a
TIDBA	4.8	4.6
TIDBAc	6	5.3
TIDBIBA	21	17.3
TIDBTMAc	44	37
TID-BE	134	123

^a Data for TID taken from Ref. 14.

Characterization of $[^{125}\text{I}]\text{TID}$ Analog Photoincorporation into AChR Subunits—Initial photolabeling experiments with each $[^{125}\text{I}]\text{TID}$ analog were designed to characterize the extent of photoincorporation into AChR subunits (*i.e.* subunit labeling pattern), as well as to assess the extent to which the addition of agonist and conformational change to the desensitized state of the AChR effects the extent of $[^{125}\text{I}]\text{TID}$ analog photoincorporation into receptor subunits (*i.e.* agonist sensitivity of $[^{125}\text{I}]\text{TID}$ photoincorporation into AChR subunits). AChR-rich membranes were equilibrated with a given $[^{125}\text{I}]\text{TID}$ analog ($\sim 1.6 \mu\text{M}$) in the absence and presence of $400 \mu\text{M}$ carbamylcholine, exposed to UV light (365 nm), and the membrane suspensions pelleted. The extent of photoincorporation into AChR subunits was monitored by autoradiography following SDS-PAGE of the solubilized membrane pellets. As is evident in the autoradiographs shown in Fig. 3, there is significant photoincorporation of each $[^{125}\text{I}]\text{TID}$ analog into the AChR α -, β -, γ -, and δ -subunits. In the resting state AChR the extent of $[^{125}\text{I}]\text{TIDBA}$ photoincorporation in receptor subunits (Fig. 3A) is indistinguishable from that of $[^{125}\text{I}]\text{TID}$ (18), including a greater amount of photoincorporation into the γ -subunit relative to the α -, β -, or δ -subunits. Furthermore, addition of agonist leads to a substantial reduction in the extent of $[^{125}\text{I}]\text{TIDBA}$ photoincorporation into each subunit (Fig. 3A, + lane). Next, for the TID analog $[^{125}\text{I}]\text{TIDBIBA}$, the extent of photoincorporation into each subunit in the resting state AChR (Fig. 3B, - lane) appears similar to that of $[^{125}\text{I}]\text{TIDBA}$ (Fig. 3A, - lane), and the addition of agonist (Fig. 3B, + lane) also results in a significant reduction in the extent $[^{125}\text{I}]\text{TIDBIBA}$ photoincorporation into each receptor subunit. However, compared with $[^{125}\text{I}]\text{TIDBA}$ (Fig. 3A), for $[^{125}\text{I}]\text{TIDBIBA}$ (Fig. 3B) there appears to be less of a difference in the extent of photoincorporation into each AChR subunit when the receptor is labeled in the absence of agonist (Fig. 3B, - lane) compared with the presence of agonist (Fig. 3B, + lane). Finally, for the TID analog $[^{125}\text{I}]\text{TIDBTMAc}$, when the photolabeling is done in the absence of agonist (Fig. 3C, - lane), the extent of photoincorporation into each AChR subunit is approximately equal, that is there is not a greater extent of labeling in the γ -subunit relative to the α -, β -, or δ -subunits as observed for TID, TIDBA, TIDBAc, and TIDBIBA. Furthermore, the extent of photoincorporation into each AChR subunit is the same whether the photolabeling is done in the absence of agonist (Fig. 3C, - lane) or in the presence of agonist (Fig. 3C, + lane).

Differences in the extent of photoincorporation by TID analogs into AChR subunits were quantified by γ -counting of excised gel bands. In the absence of agonist, the 4-fold greater magnitude of photoincorporation into the γ -subunit relative to the other AChR subunits by $[^{125}\text{I}]\text{TID}$ is maintained for the

analogs [125 I]TIDBA, [125 I]TIDBAc, and [125 I]TIDBIBA. For these same analogs, however, there is a progressive reduction in the extent of photoincorporation into AChR subunits for photolabeling experiments done in the absence *versus* in the presence of agonist, *i.e.* reduction in the agonist sensitivity of subunit labeling (summarized in Table II). Furthermore, for [125 I]TIDBTMAc and [125 I]TID-BE, there is actually a reversal in the agonist sensitivity such that there is a slightly greater amount of TID analog photoincorporation into each AChR subunit for labeling experiments done in the presence of agonist compared with the resting state.

The differences in the extent of photoincorporation of [125 I]TID analogs into AChR subunits for receptors labeled in

the absence and presence of agonist were further characterized by proteolytic mapping. For AChRs photolabeled with a given [125 I]TID analog, in each case the labeled AChR α -subunit (– and + carbamylcholine labeling condition) was partially digested using *S. aureus* V8 protease under Cleveland gel conditions (10, 20, 25). Cleveland gel analysis of the AChR α -subunit generates four large, non-overlapping fragments of the α -subunit allowing the distribution of 125 I cpm within the subunit to be determined. For each of the [125 I]TID analogs, photoincorporation in the AChR α -subunit was found to be restricted to two V8 protease fragments, α V8–20 (Ser-173–Glu-338) and α V8–10 (Asn-339–Gly-437; data not shown). The stretch of the primary sequence of the α -subunit contained within the V8 protease fragment α V8–20 includes the transmembrane segments M1, M2, and M3; the fragment α V8–10 contains the transmembrane segment M4. The extent of [125 I]TID analog photoincorporation into the V8 protease fragments α V8–20 and α V8–10 for AChRs labeled in the absence and presence of agonist is summarized in Table III. Previous studies with [125 I]TID have shown that, for AChRs labeled in the absence of agonist, the bulk of the photoincorporation into α V8–20 reflects labeling of amino acid residues in the M2 segment (14, 16). Consistent with this, we found that for AChRs photolabeled with [125 I]TID in the absence of agonist, that is the resting state of AChR, approximately 81% of the total [125 I]TID photoincorporation into the α -subunit is localized within the V8 protease fragment α V8–20 and 19% is found in α V8–10 (Table III). In contrast, for AChRs photolabeled with [125 I]TID in the presence of agonist, that is the desensitized state, only 47% of the total photoincorporation into the α -subunit is in α V8–20 and 53% is in α V8–10. For AChRs photolabeled in the resting state, 80% of the total photoincorporation into the α -subunit is localized to α V8–20 for the TID analog [125 I]TIDBA, 73% for [125 I]TIDBIBA, and ~40% for [125 I]TIDBTMAc and [125 I]TID-BE (Table III).

When the distribution of 125 I cpm within the α -subunit was determined for AChRs labeled with each of the [125 I]TID analogs in the desensitized state, photoincorporation into both V8 protease fragments as a percentage of the total are approximately equivalent (Table III). In addition, although not presented in Table III, the extent of photoincorporation of each [125 I]TID analog into the V8 protease fragment α V8–10 was

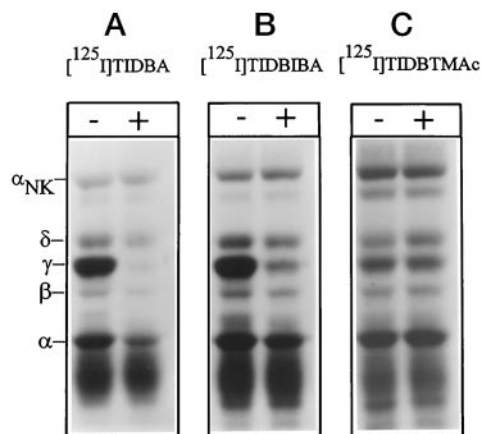


FIG. 3. Photoincorporation of [125 I]TIDBA, [125 I]TIDBIBA, and [125 I]TIDBTMAc into AChR-rich membranes in the resting and desensitized state of the AChR. AChR-rich membranes were equilibrated (2-h incubation) with either [125 I]TIDBA, [125 I]TIDBIBA or [125 I]TIDBTMAc (~1.6 μ M) in the absence (– lane) and in the presence (+ lane) of 400 μ M carbamylcholine (agonist) and then irradiated at 365 nm (Spectroline EN-280L) for 7 min (at a distance of <1 cm). Polypeptides were resolved by SDS-PAGE (1.0-mm thick, 8% polyacrylamide gel), visualized by Coomassie Blue R-250 staining, and subjected to autoradiography (1–2-day exposure with intensifying screen). Labeled lipid and free photolysis products were electrophoresed from the gel with the tracking dye. The migration of individual AChR subunits is indicated on the left. The percent photoincorporation of each [125 I]TID analog into each receptor subunit in the resting *versus* desensitized state of the AChR is shown in Table II.

TABLE II

Percent photoincorporation of [125 I]TID analog into each AChR subunit in the resting *versus* desensitized state of the AChR

The amount of photoincorporation of each [125 I]TID analog (cpm) into each AChR subunit is expressed as the ratio of photoincorporation observed when the labeling was conducted under conditions that favor the resting *versus* desensitized state of the AChR (see “Experimental Procedures”). For TIDBTMAc and TID-BE the upward-pointing arrows indicate a greater amount of photoincorporation in the desensitized state compared with that determined in the resting state of the AChR ($n = 8$).

	[125 I]TID	[125 I]TIDBA	[125 I]TIDBAc	[125 I]TIDBIBA	[125 I]TIDBTMAc	[125 I]TID-BE
α	75	41	34	25	14 \uparrow	10 \uparrow
β	88	40	28	23	20 \uparrow	30 \uparrow
γ	95	82	74	72	3 \uparrow	3 \uparrow
δ	80	30	18	13	18 \uparrow	13 \uparrow

TABLE III

Percent photoincorporation of [125 I]TID analog into the *S. aureus* V8 protease cleavage fragments of the AChR α -subunit (α V8–20/ α V8–10)

[125 I]TID analog photoincorporation into each V8 fragment was determined in the resting state and in the desensitized state of the AChR. For each [125 I]TID analog, the AChR α -subunit was isolated under photolabeling conditions that favor either the resting or desensitized state of the AChR. The isolated α -subunit was proteolytically digested with *S. aureus* V8 protease under Cleveland gel conditions (10, 25). For each [125 I]TID analog photoincorporation was restricted to two V8 protease fragments: α V8–20 (Ser-173–Glu-338) and α V8–10 (Asn-339–Gly-437) and which contain the membrane-spanning segments M1–M3 and M4, respectively. α V8–20 contains the channel-lining M2 segment, and α V8–10 contains the M4 segment which is situated at the lipid-protein interface (10, 20). The amount of [125 I]TID analog photoincorporation into each fragment was determined, and the data are presented as the percent photoincorporation into α V8–20 compared with α V8–10 (*i.e.* 81/19).

	[125 I]TID	[125 I]TIDBA	[125 I]TIDBIBA	[125 I]TIDBTMAc	[125 I]TID-BE
Resting state	81/19	80/20	73/27	41/59	40/60
Desensitized state	47/53	47/53	47/53	46/54	46/54

nearly identical for AChRs labeled in the absence and in the presence of agonist. Previous work has established that the majority of photoincorporation of [125 I]TID and [125 I]TID-BE into the fragment α V8–20 (in desensitized state AChR) and into α V8–10 (labeled in the resting and desensitized state of the AChR) reflects labeling of amino acids in the transmembrane segments M1, M3, and M4 (10, 19, 20). For the fragment α V8–20, there is photoincorporation into amino acids in the transmembrane segments M1 and M3, and for α V8–10, photoincorporation into amino acids within M4. It was further concluded that these amino acids are in contact with lipid, with the AChR transmembrane segments M1, M3, and M4 comprising the lipid-protein interface of the receptor. The simplest interpretation of the α -subunit mapping results for each [125 I]TID analog is as follows: 1) that agonist-sensitive photoincorporation within the V8 fragment α V8–20 reflects labeling of amino acids in the α M2 segment; 2) that photoincorporation into the V8 fragment α V8–10 and the bulk of photoincorporation into α V8–20 for desensitized state AChRs reflects labeling of amino acid residues in the transmembrane segments M1, M3, and M4 that are in contact with lipid.

Inhibition of [125 I]TID Analog Photoincorporation into the AChR Channel in the Resting State by the Noncompetitive Antagonists TMB-8 and Tetracaine—To confirm that the differences in the agonist sensitivity of [125 I]TID analog photoincorporation into AChR subunits is truly a reflection of differences in the extent of photoincorporation into the resting state channel, we tested the ability of NCAs that bind to the AChR channel in the resting state to inhibit [125 I]TID analog photoincorporation into receptor subunits.² The local anesthetic tetracaine binds with high affinity ($K_{eq} = 0.3 \mu\text{M}$) to a single site in the resting state AChR, and this site has been localized by photoaffinity labeling to the M2 segment of each receptor subunit that together comprise the resting state channel (11, 12). TMB-8 (3,4,5-trimethoxybenzoic acid 8-(diethylamino) octyl ester) binds with equal affinity to the AChR channel in both its resting and desensitized states and has been shown to inhibit competitively [125 I]TID photoincorporation into AChR subunits in the resting state ($IC_{50} = 3.1 \mu\text{M}$ (10)).

As shown in Fig. 4A, [125 I]TIDBIBA photoincorporation into each AChR subunit in the resting state is reduced in a concentration-dependent fashion by co-equilibration with TMB-8. At 50 μM TMB-8 (Fig. 4, 7th lane), the level of [125 I]TIDBIBA photoincorporation into AChR subunits is reduced nearly to that observed in the presence of agonist (Fig. 4, 8th lane). The concentration-response curve for TMB-8 and [125 I]TIDBIBA is shown in Fig. 4B and overlaps that for [125 I]TID resulting in very similar IC_{50} values (3.6 and 3.1 μM respectively; Table IV). Similar IC_{50} values were also calculated for TMB-8 inhibition of [125 I]TIDBA and [125 I]TIDBAc photoincorporation into AChR subunits in the resting state (Table IV). In contrast, whereas 50 μM TMB-8 reduced [125 I]TIDBIBA photoincorporation into the γ -subunit by greater than 98%, it had no effect (less than 5% reduction) on the extent of photoincorporation of [125 I]TIDBTMAc into the γ -subunit (Fig. 4B; Table IV). TMB-8 eliminates the majority of photoincorporation into AChR subunits for the [125 I]TID analogs TID, TIDBA, TIDBAc, and TIDBIBA but not for TIDBTMAc and TID-BE. These results further substantiate the conclusion that the agonist-sensitive

² In addition to the NCAs listed in Table IV, the following compounds were also tested as inhibitors of [125 I]TID photoincorporation into the resting state AChR (IC_{50} values in micromolar are in parentheses): propofol (48); adifenine (2.1); amobarbital (7.8); pentobarbital (143); secobarbital (123); phenobarbital (362); butalbarbital (516), and barbital (1800). In contrast the dissociative anesthetic ketamine produced a 52% increase in the extent of [125 I]TID photoincorporation into the resting state AChR ($EC_{50} = 16 \mu\text{M}$).

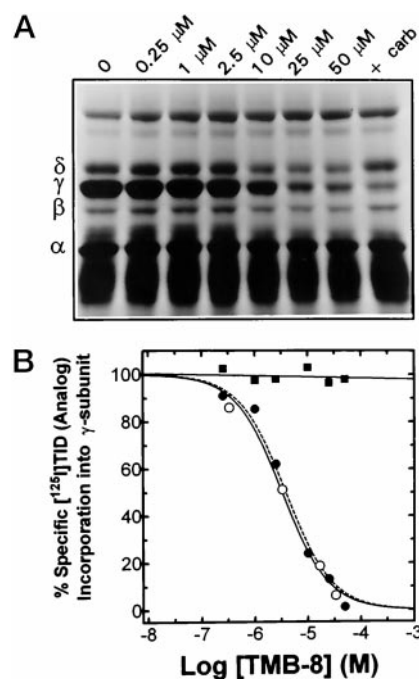


FIG. 4. The effect of the noncompetitive antagonist TMB-8 on the photoincorporation of [125 I]TIDBIBA into AChR-rich membranes. AChR-rich membranes were equilibrated (2 h) with [125 I]TIDBIBA ($\sim 1.6 \mu\text{M}$) in the absence (1st to 7th lanes) and in the presence (8th lane) of 400 μM carbamylcholine (agonist) or in the presence of increasing concentrations of the AChR noncompetitive antagonist TMB-8 (2nd to 7th lanes). AChR-rich membranes were then irradiated at 365 nm for 7 min, and polypeptides were resolved by SDS-PAGE. A, shown is the corresponding autoradiograph of the gel containing the competition labeling experiment [125 I]TIDBIBA versus TMB-8. The positions of the AChR subunits are indicated on the left. B, for each [125 I]TID analog versus TMB-8 competition labeling experiment, individual AChR subunit bands were excised from the dried gel, and the amount of [125 I]TID analog photoincorporated into each subunit determined by gamma counting. The data points for [125 I]TIDBIBA (\bullet), [125 I]TID (\circ), and [125 I]TIDBTMAc (\blacksquare) photoincorporation into the AChR γ -subunit are shown and were calculated as described under "Experimental Procedures." For [125 I]TIDBIBA and [125 I]TID the solid and dashed lines represent, respectively, the nonlinear least squares fit of each of the binding data sets. The IC_{50} values calculated from these curves are shown in Table IV. For [125 I]TIDBTMAc, photoincorporation into the γ -subunit was expressed simply as a percentage of the amount of photoincorporation determined in the absence of any other drug. No significant ($>10\%$) difference in the extent of [125 I]TIDBTMAc photoincorporation into the γ -subunit was detected at any concentration of TMB-8.

(TMB-8 inhibitable) photoincorporation of the [125 I]TID analogs (TID, TIDBA, TIDBAc, and TIDBIBA) into AChR subunits represents photoincorporation into the resting state channel at a single or overlapping binding site(s). The results of tetracaine inhibition of [125 I]TID analog photoincorporation into the resting state AChR also support this conclusion. Tetracaine and [125 I]TID bind to the resting state channel in a mutually exclusive manner, and the sites of [^3H]tetracaine and [125 I]TID photoincorporation in the M2 segments of each subunit overlap (11, 12). As shown in Table IV, tetracaine completely eliminates agonist-inhibitable photoincorporation into AChR subunits in the resting state for the [125 I]TID analogs TIDBA and TIDBIBA with IC_{50} values (0.89, 1.1 μM). These IC_{50} values are very similar to the values determined for inhibition of [125 I]TID photoincorporation into AChR subunits (1.02 μM (17)).

Identification of the Sites of [125 I]TIDBIBA Photoincorporation into δ -M2—Previous results demonstrate that the agonist-inhibitable, NCA-displaceable [125 I]TID analog photoincorporation into subunits of the resting state AChR is localized to the channel. These results, however, leave open the possibility that

TABLE IV
Calculated IC_{50} values for drug blockage of [^{125}I]TID analog photoincorporation into the resting state AChR γ -subunit

The IC_{50} values (concentration at which drug reduces [^{125}I]TID analog photoincorporation into the γ -subunit of the AChR by 50% of the maximal effect) were determined by nonlinear least squares analysis. [^{125}I]TID analog labeling of the resting state of the AChR is described under "Experimental Procedures."

Drug	IC_{50}					
	[^{125}I]TID	[^{125}I]TIDBA	[^{125}I]TIDBAc	[^{125}I]TIDBIBA	[^{125}I]TIDBTMAc	[^{125}I]TID-BE
TMB-8	3.1	2.75	2.67	3.6	No effect	No effect
Tetracaine	1.02	0.89		1.1		No effect

the [^{125}I]TID and the [^{125}I]TID analogs bind to unique but overlapping sites in the resting channel. Indirect evidence of a common binding locus comes from the pattern of photoincorporation into subunits in the resting state AChR. In the resting state AChR, [^{125}I]TID photoincorporates into the γ -subunit at a 4-fold greater level than into the α -, β -, or δ -subunits. The increased photoincorporation into the γ -subunit by [^{125}I]TID is a consequence of highly efficient photoincorporation into a single amino acid, Ile-264 (position 13) of the γ M2 segment (16). The 4-fold greater labeling of the γ -subunit compared with the other AChR subunits is maintained for photoincorporation of [^{125}I]TIDBA, [^{125}I]TIDBAc, and [^{125}I]TIDBIBA into receptor subunits. This indicates that Ile-264 is also the primary site of photoincorporation in γ M2 for each of these TID analogs, and it further suggests a common binding locus in the resting state channel. However, in order to resolve this issue more completely, we wished to determine the amino acids that are photolabeled by [^{125}I]TIDBIBA in the M2 segment of the δ -subunit. We chose to determine the site(s) of [^{125}I]TIDBIBA photoincorporation into δ M2 for several reasons as follows: (a) because [^{125}I]TID photoincorporates into δ Leu-265 and δ Val-269 within δ M2 to an approximately equal extent (16); (b) technically δ M2 is the easiest M2 segment to isolate, γ M2 being the most difficult to isolate and is prone to irreversible aggregation (13); (c) because the amino acids photolabeled by [^{125}I]TID-BE in the δ M2 segment have also been determined. AChR-rich membranes (10 mg per condition) were labeled with [^{125}I]TIDBIBA (3 μ M) in the absence and presence of carbamylcholine. The δ -subunits isolated from each condition were digested with 20% (w/w) trypsin for 4 days. The digests were resolved by Tricine SDS-PAGE, and a 5-kDa fragment (δ T-5K) known to contain the M2-M3 region (16, 13) was isolated from the gel as described under "Experimental Procedures." The δ T-5K fragment was further purified by reversed-phase HPLC (Fig. 5A), and for each labeling condition the majority of [^{125}I] cpm eluted in a peak centered at 98% solvent B. HPLC fractions 36–39, for δ T-5K isolated from resting state AChRs (Fig. 5A, ●), were pooled and subjected to amino-terminal amino acid sequence analysis (Fig. 5B). Sequence analysis revealed the presence of a single sequence, present at a 10-fold or greater level than any secondary sequence, beginning at δ Met-257 at the amino terminus of δ M2. The primary site of [^{125}I] release occurred in cycle 13 with a small amount of release also present in cycle 9 (Fig. 5B, ●). These results indicate that within the δ M2 segment and in the resting state AChR, [^{125}I]TIDBIBA photoincorporates into δ Leu-265 (0.71 cpm/pmol) and δ Val-269 (5.2 cpm/pmol). These same two residues are also the primary sites of [^{125}I]TID photoincorporation into δ M2 in the resting state AChR (16). Whereas both compounds photoincorporate into the same two δ M2 residues, [^{125}I]TID photoincorporates into δ Val-269 at \sim 2-fold greater efficiency than into δ Leu-265, whereas [^{125}I]TIDBIBA photoincorporates into δ Val-269 at \sim 7-fold greater efficiency than into δ Leu-265. These results establish that [^{125}I]TID and [^{125}I]TIDBIBA share the same binding locus in the resting state channel; as for the differences in efficiency of

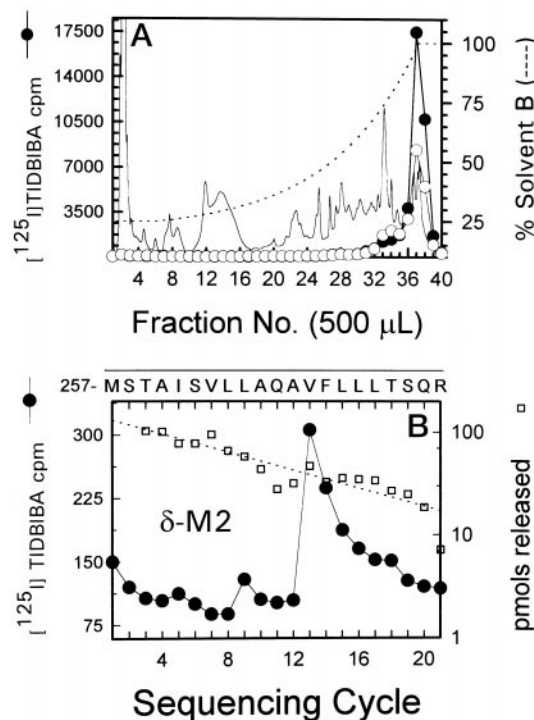


FIG. 5. Reverse-phase HPLC purification and sequential Edman degradation of a [^{125}I]TIDBIBA-labeled fragment containing δ M2. The [^{125}I]TIDBIBA-labeled AChR δ -subunit isolated from AChRs labeled in the resting state (●) and desensitized state (○) were further digested in solution with trypsin, and an approximately 5-kDa (δ T-5K) fragment was isolated from a 1.5-mm thick 16.5% T, 6% C Tricine gel (see "Experimental Procedures"). The labeled material was further purified by reverse-phase HPLC (A) on a Brownlee Aquapore C₄ column (100 \times 2.1 mm) as described under "Experimental Procedures." The elution of peptides was monitored by absorbance at 210 nm (solid line) and elution of [^{125}I] by γ -counting of each 500 μ l fraction (●, ○). For each condition, HPLC fractions 36–39 were pooled and subjected to automated sequential Edman degradation. B, shown is the radiosequencing profile for the δ T-5K fragment that contains the M2 segment of the δ -subunit isolated from AChRs labeled in the resting state. Eighty percent of each cycle of Edman degradation was analyzed for released [^{125}I] (●) and 20% for released PTH-derivatives (□) with the dashed line corresponding to the exponential decay fit of the amount of detected PTH-derivatives. A primary peptide was detected beginning at Met-257 of the δ -subunit (initial yield, 130 pmol; repetitive yield, 89.9%; 15,495 cpm loaded on sequencing filter; 6,477 cpm remaining after 20 cycles). The amino acid sequence of the peptide is shown above B with the solid line indicating the limits of the M2 region.

photoincorporation into amino acids in the δ M2 segment, one interpretation is that the binding of [^{125}I]TIDBIBA is more restricted (*i.e.* reduced mobility and/or orientation) compared with that of [^{125}I]TID. δ Val-269 being the principal site of [^{125}I]TIDBIBA photoincorporation in the δ M2 segment is then a result of TIDBIBA adopting a preferred orientation in the resting state channel.

HPLC fractions 36–39 for δ T-5K isolated from desensitized state AChRs (Fig. 5A, ○) were also pooled and subjected to

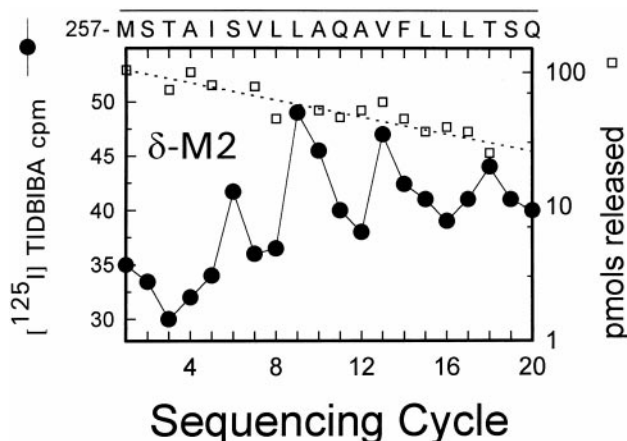


FIG. 6. Radioactivity and mass release upon amino-terminal sequencing analysis of a [^{125}I]TIDBIBA-labeled fragment containing δM2 isolated from desensitized state AChRs. The [^{125}I]TIDBIBA-photolabeled AChR δ -subunit isolated from desensitized state AChRs was further digested in solution with trypsin, and an approximately 5-kDa ($\delta\text{T-5K}$) fragment was isolated from a 1.5-mm thick 16.5% T, 6% C Tricine gel and further purified by reverse-phase HPLC (Fig. 5A). HPLC fractions 36–39 for $\delta\text{T-5K}$ isolated from desensitized state AChRs (Fig. 5A, \circ) were pooled and subjected to automated sequential Edman degradation. Shown is the radiosequencing profile for the $\delta\text{T-5K}$ fragment that contains the M2 segment of the δ -subunit isolated from desensitized state AChRs. Eighty percent of each cycle of Edman degradation was analyzed for released ^{125}I (\bullet) and 20% for released PTH-derivatives (\square) with the dashed line corresponding to the exponential decay fit of the amount of detected PTH-derivatives. A primary peptide was detected beginning at Met-257 of the δ -subunit (initial yield, 112 pmol; repetitive yield, 92.6%; 8,417 cpm loaded on sequencing filter; 2,805 cpm remaining after 20 cycles). The amino acid sequence of the peptide is shown above the panel with the solid line indicating the limits of the M2 region.

amino-terminal amino acid sequence analysis (Fig. 6). As with $\delta\text{T-5K}$ isolated from resting state AChRs, sequence analysis revealed the presence of a single sequence, present at a ~ 10 -fold greater level than any secondary sequence. The primary sequence began at $\delta\text{Met-257}$, the amino terminus of the δM2 segment. The ^{125}I cpm release profile was somewhat complex but indicated a small amount of release occurring in cycles 6, 9, 13, and possibly cycle 18 (Fig. 6, \bullet). Release in these cycles corresponds to [^{125}I]TIDBIBA photoincorporation into $\delta\text{Ser-262}$ (0.11 cpm/pmol), $\delta\text{Leu-265}$ (0.21 cpm/pmol), $\delta\text{Val-269}$ (0.19 cpm/pmol), and $\delta\text{Thr-265}$ (0.10 cpm/pmol). These same amino acids were determined to be the primary sites of [^{125}I]TID photoincorporation into δM2 in the desensitized state AChR (16), indicating that TID and TIDBIBA bind to the same locus in the desensitized state channel. In contrast, based upon [^{125}I]TID-BE photoincorporation into $\beta\text{Leu-257}$, $\beta\text{Val-261}$, and $\beta\text{Leu-264}$ in the βM2 segment, it was concluded that compared with TID, TID-BE binds to a unique but overlapping site in the desensitized state channel. The binding locus for TID-BE appears to be located slightly higher in the channel, toward the extracellular side of the membrane (10).

Finally, the interaction of TIDBIBA with the AChR channel in the desensitized state was further assessed by examining the effect of TIDBIBA on the binding of [^3H]thienyl-cyclohexylpiperidine ([^3H]TCP) to AChR membranes. [^3H]TCP binds with high affinity to the AChR channel in the desensitized state (26), and binding assays were done exactly as in Ref. 13. TIDBIBA was found to inhibit [^3H]TCP binding to the desensitized state AChR with an IC_{50} value of $9\ \mu\text{M}$ ($n_{\text{H}} = 0.92$). TIDBTMAc also inhibited [^3H]TCP binding to the desensitized state AChR but with a weaker potency ($\text{IC}_{50} = 17\ \mu\text{M}$; $n_{\text{H}} = 0.87$). TCP is a close structural analog of phencyclidine (PCP), and the binding of [^3H]TCP and [^3H]PCP to the desensitized

state AChR is virtually indistinguishable (26).³ TID was previously shown to inhibit [^3H]PCP binding to the desensitized state AChR with a K_i of $2\ \mu\text{M}$ (14).

DISCUSSION

The goal of this work was to gain insight into the molecular determinants of NCA binding to the channel of the AChR in the resting state. Our strategy for achieving this goal involved employing a series of analogs of the potent AChR NCA, [^{125}I]TID. The binding site for TID in the AChR channel in the resting state has been well characterized. TID binds with unitary stoichiometry and micromolar affinity to the resting state channel, photoincorporating into homologous aliphatic residues at positions 9 and 13 (e.g. $\beta\text{Leu-257}$ and $\beta\text{Val-261}$) of each M2 segment (14–16). We assessed the ability of analogs of TID (Fig. 1) to interact with the NCA-binding site in several ways as follows: 1) the ability of a nonradioactive TID analog to inhibit competitively [^{125}I]TID photoincorporation into AChR subunits in the resting state; 2) the pattern and agonist sensitivity of [^{125}I]TID analog photoincorporation into AChR subunits; 3) the ability of NCAs that are known to interact with the resting state channel to inhibit competitively photoincorporation of a given [^{125}I]TID analog into subunits of the AChR in the resting state. The first TID analog we tested, TIDBA (Fig. 1), has a primary alcohol group attached to the TID benzene ring (position 1) and provided a critical test as to what effect even a small addition to the TID molecule would have upon its interaction with the NCA site. As judged by the criteria established above, the interaction of TIDBA with the NCA site in the resting state channel is nearly indistinguishable from that of TID itself. TIDBA inhibits [^{125}I]TID photoincorporation into AChR subunits in the resting state in a concentration-dependent fashion. A concentration of $50\ \mu\text{M}$ TIDBA inhibited [^{125}I]TID photoincorporation into the γ -subunit by greater than 98%, and from the entire concentration range that was tested an IC_{50} value of $4.8\ \mu\text{M}$ was calculated. This value is nearly identical to that of nonradioactive TID inhibition of [^{125}I]TID photoincorporation (Fig. 2 and Table I). Next, the extent of [^{125}I]TIDBA photoincorporation into each AChR subunit (subunit labeling pattern) and the effect of the addition of agonist on the extent of photoincorporation into receptor subunits (agonist sensitivity) for [^{125}I]TIDBA are nearly identical to that of [^{125}I]TID (Fig. 3A and Table II). Finally, the NCAs tetracaine and TMB-8 that bind to the (TID) NCA site in the resting state channel completely displace specific [^{125}I]TIDBA photoincorporation into the AChR subunits in the resting state with nearly identical IC_{50} values compared with [^{125}I]TID (Table IV).

We next converted the alcohol function of TIDBA into either an acetate, isobutyl acetate, or trimethyl acetate group (TIDBAc, TIDBIBA, or TIDBTMAc, respectively; Fig. 1). For these TID analogs there was a progressive rightward shift in the concentration-response curves for inhibition of [^{125}I]TID photoincorporation into AChR subunits in the resting state, resulting in 1.5-, 5.25-, and 11-fold decreases in potencies (Table I). This decrease in the ability of a given concentration of TID analog to inhibit [^{125}I]TID photoincorporation into the resting state channel parallels a decrease in the agonist sensitivity of [^{125}I]TID analog photoincorporation into AChR subunits (Fig. 3 and Table II). For [^{125}I]TID, the addition of agonist (desensitized state of AChR) results in an $\sim 95\%$ decrease in the extent of photoincorporation into the γ -subunit. This decrease in photoincorporation into the γ -subunit (as well as the α -, β -, and δ -subunits) is a result of decreased efficiency of [^{125}I]TID photoincorporation into amino acids in the M2 segment that results from an agonist-induced change in the structure of the

³ M. P. Blanton, unpublished data.

channel and the NCA site (16). For the analog [125 I]TIDBIBA, addition of agonist results in only a 72% reduction in photoincorporation into the γ -subunit, and for [125 I]TIDBTMAc there is actually a very small increase in the extent of photoincorporation in the presence of agonist (Table II). The simplest interpretation of these results is that there is a progressive reduction in the ability of each TID analog as cited to interact with the NCA site in the resting state channel. In other words, each consecutive TID analog has a reduced affinity for binding to the resting state channel and a reduced ability to photoincorporate efficiently into amino acids within the NCA site. There are several lines of evidence that support this interpretation. First, there is both direct and indirect evidence that the TID analogs are binding to a common site within the resting state channel. In resting state AChR, [125 I]TID photoincorporates into the γ -subunit at a 4-fold greater level than into the α -, β -, or δ -subunits. The greater extent of photoincorporation of [125 I]TID into the γ -subunit relative to the α -, β -, or δ -subunits is a consequence of highly efficient photoincorporation into a single amino acid, Ile-264 (position 13) of the γ M2 segment (16). This 4-fold greater photoincorporation into the γ -subunit is maintained for photoincorporation into the AChR subunits by [125 I]TIDBA, [125 I]TIDBAc, and [125 I]TIDBIBA. The simplest interpretation of these results is that γ Ile-264 is also the primary site of photoincorporation in the γ M2 segment for each of these [125 I]TID analogs and that they share a common binding site in the resting state channel. Direct evidence of a common binding site comes from the determination that the sites of [125 I]TIDBIBA photoincorporation in the channel-lining δ M2 segment (δ Leu-265, δ Val-269) are identical to those previously determined for [125 I]TID (Fig. 5B (16)). Next, previous work has established that the addition of AChR agonist (carbamylcholine) or NCAs such as tetracaine or TMB-8 reduces by greater than 75% the photoincorporation of [125 I]TID into receptor subunits (16, 17). Furthermore, the inhibition of [125 I]TID photoincorporation into AChR subunits by either NCAs or addition of agonist has been shown to reflect identical reductions in the extent of [125 I]TID photoincorporation into amino acids in the M2 segment of each receptor subunit (14, 16, 17). Nearly identical IC₅₀ values are obtained from the concentration-response curves for TMB-8 inhibition of [125 I]TID, [125 I]TIDBA, [125 I]TIDBAc, and [125 I]TIDBIBA photoincorporation into AChR subunits, and the same is true for tetracaine (Table IV). These results suggest a common binding site for each of the TID analogs and for tetracaine and TMB-8 in the AChR channel in the resting state.

Focusing on the TID analogs [125 I]TIDBIBA and [125 I]TIDBTMAc, it is evident that the additional methyl group of TIDBTMAc (Fig. 1) results in the following: 1) a 2-fold further reduction in the potency by which TIDBTMAc inhibits [125 I]TID photoincorporation into AChR subunits in the resting state, compared with TIDBIBA, and 2) a complete loss of agonist-sensitive, NCA-inhibitable photoincorporation into AChR subunits. Comparison of the CPK structures of TIDBIBA and TIDBTMAc (not shown) indicate that the additional methyl group of TIDBTMAc appears to contribute only a very small amount of additional mass. Nevertheless, this additional bulk results in a 2-fold decrease in the binding affinity to the NCA site in the resting state channel and a complete loss of any detectable photoincorporation into the resting state channel. If TIDBIBA or TIDBTMAc are placed in the resting state channel (27) with the photoreactive diazirine group positioned adjacent to δ Val-269 (the primary site of [125 I]TIDBIBA photoincorporation in δ M2), the additional bulk of TIDBTMAc is then in approximate register with δ Leu-265, located one turn of the δ M2 α -helix lower in the channel. Structural studies of the

AChR suggest that in the resting state channel δ Leu-265 as well as the leucine residue at this position (position 9) in the M2 segment in each of the other subunits are in close proximity to one another and together form a restriction, or gate, to ion permeation (16, 28, 29). Whereas the channel-lining M2 segments are predominantly α -helical, structural studies (28, 29) suggest that each M2 helix has a central kink around position 9 (*e.g.* δ Leu-265). The kink in the M2 helix results in a narrowing of the channel at this position, bringing the side chains of each conserved leucine residue in close apposition to one another (27). The narrowing of the channel at this position and the close apposition of the aliphatic side chains of each leucine residue in all likelihood provides an ideal binding site for uncharged NCAs such as TID as well as diazofluorene (13). On the other hand, the restriction in the lumen of the channel is also likely to present a progressively greater amount of steric hindrance to the binding of each of the TID analogs, TIDBA, TIDBAc, TIDBIBA, TIDBTMAc, and TID-BE, in which an increasingly bulkier substituent has been added to the TID parent compound. For TIDBTMAc and TID-BE the affinity for the NCA site in the resting state channel and the efficiency of photoincorporation into M2 residues are so reduced that labeling of the resting state channel is not apparent at the level of the intact subunit. However, close examination of the sites of [125 I]TID-BE photoincorporation into AChR subunits in the absence of agonist (see Fig. 6 in Ref. 10)³ reveals a very small amount of photoincorporation into β Val-261 (0.48 cpm/pmol) in β M2 and into δ Val-269 (0.55 cpm/pmol) in δ M2. The extent of [125 I]TID-BE photoincorporation into δ Val-269 is, however, one-tenth that of [125 I]TIDBIBA (5.2 cpm/pmol, under very similar labeling conditions). These results are consistent with a model of the NCA site in the resting state channel in which the restriction in the lumen of the channel (at position 9 of each M2 helix) presents substantial steric hindrance to the binding of the more bulky TID analogs (*e.g.* TIDBTMAc and TID-BE).

Finally, a recent study (12) determining the sites of [3 H]tetracaine photoincorporation in the M2 segments of the AChR in the resting state suggest that the restriction in the lumen of the channel (at position 9 of each M2 segment) is somewhat flexible. [3 H]Tetracaine photoincorporates into Ile-247 (position 5), Leu-251 (position 9), and Val-255 (position 13) in the α M2 segment. [3 H]Tetracaine photoincorporation into Ile-247 in α M2 places at least a portion of the tetracaine molecule below the apparent restriction in the lumen of the channel at position 9. This fact and that the kinetics of tetracaine binding to the resting state AChR are characterized by a very low association rate constant led the authors (Gallagher and Cohen (12)) to conclude that the restriction in the pore of the resting state channel relaxes somewhat in order to accommodate the binding of tetracaine. The authors further suggest that the dimethylamino group of tetracaine interacts with Ser-248 (position 6) in α M2 providing energetic stability to tetracaine binding to the resting state channel. Synthesis of additional TID analogs, including analogs that contain a dimethylamino substituent, as well as molecular modeling studies will undoubtedly yield a more complete picture of the NCA site in the resting state channel and of the molecular determinants of NCA binding.

Acknowledgments—We thank Dr. Josef Brunner (Swiss Federal Institute of Technology Zurich, Zurich, Switzerland) for kindly providing the tin precursors TIDBA and TID-BE. We thank Dr. Jay Ponder (Washington University School of Medicine, St. Louis, MO) for use of the computer workstation, molecular graphics software, and invaluable assistance. Finally we thank Drs. Mark Sansom and Graham Smith (University of Oxford, Oxford, UK) for kindly providing the coordinates for their kinked α 7 M2 molecular model.

REFERENCES

1. Hucho, F., Tsetlin, V. I., and Machold, J. (1996) *Eur. J. Biochem.* **239**, 539–557
2. Arias, H. R. (1997) *Brain Res. Rev.* **25**, 133–191
3. Unwin, N. (1998) *J. Struct. Biol.* **121**, 181–190
4. Arias, H. R. (1998) *Biochim. Biophys. Acta* **1376**, 173–220
5. Giraudat, J., Dennis, M., Heidmann, T., Chang, J., and Changeux, J. P. (1986) *Proc. Natl. Acad. Sci. U. S. A.* **83**, 2719–2723
6. Giraudat, J., Galzi, J.-L., Revah, F., Changeux, J.-P., Haumont, P.-Y., and Lederer, F. (1989) *FEBS Lett.* **253**, 190–198
7. Revah, F., Galzi, J.-L., Giraudat, J., Haumont, P.-Y., Lederer, F., and Changeux, J.-P. (1990) *Proc. Natl. Acad. Sci. U. S. A.* **87**, 4675–4679
8. Hucho, F. (1986) *Eur. J. Biochem.* **158**, 211–226
9. Pedersen, S. E., Sharp, S. D., Liu, W.-S., and Cohen, J. B. (1992) *J. Biol. Chem.* **267**, 10489–10499
10. Blanton, M. P., McCardy, E. A., Huggins, A., and Parikh, D. (1998) *Biochemistry* **37**, 14545–14555
11. Cohen, J. B., Medynski, D. C., and Strnad, N. P. (1985) in *Effects of Anesthesia* (Covino, G., Fozzard, H. A., Rehder, K., and Strichartz, G., eds) pp. 53–63, American Physiological Society, Bethesda
12. Gallagher, M. J., and Cohen, J. B. (1999) *Mol. Pharmacol.* **56**, 300–307
13. Blanton, M. P., Dangott, L. J., Raja, S. K., Lala, A. K., and Cohen, J. B. (1998) *J. Biol. Chem.* **273**, 8659–8668
14. White, B. H., Howard, S., Cohen, S. G., and Cohen, J. B. (1991) *J. Biol. Chem.* **266**, 21595–21607
15. Wu, G., Raines, D. E., and Miller, K. W. (1994) *Biochemistry* **33**, 15375–15381
16. White, B. H., and Cohen, J. B. (1992) *J. Biol. Chem.* **267**, 15770–15783
17. Moore, M. A., and McCarthy, M. P. (1994) *Biochim. Biophys. Acta* **1190**, 457–464
18. White, B. H., and Cohen, J. B. (1988) *Biochemistry* **27**, 8741–8751
19. Blanton, M. P., and Cohen, J. B. (1992) *Biochemistry* **31**, 3738–3750
20. Blanton, M. P., and Cohen, J. B. (1994) *Biochemistry* **33**, 2859–2872
21. Chiara, D. C., and Cohen, J. B. (1997) *J. Biol. Chem.* **272**, 32940–32950
22. Weber, T., and Brunner, J. (1995) *J. Am. Chem. Soc.* **117**, 3084–3095
23. Eichler, J., Brunner, J., and Wickner, W. (1997) *EMBO J.* **16**, 2188–2196
24. Laemmli, U. K. (1970) *Nature* **227**, 680–685
25. Cleveland, D. W., Fischer, S. G., Kirschner, M. W., and Laemmli, U. K. (1977) *J. Biol. Chem.* **252**, 1102–1106
26. Katz, E. J., Cortes, V. I., Eldefrawi, M. E., and Eldefrawi, A. T. (1997) *Toxicol. Appl. Pharmacol.* **146**, 227–236
27. Smith, G. R., and Sansom, M. S. P. (1998) *Biophys. J.* **73**, 1364–1381
28. Unwin, N. (1995) *Nature* **373**, 37–43
29. Miyazawa, A., Fujiyoshii, Y., Stowell, M., and Unwin, N. (1999) *J. Mol. Biol.* **288**, 765–786